Tailoring the Exciton Fine Structure of Cadmium Selenide Nanocrystals with Shape Anisotropy and Magnetic Field

Chiara Sinito,[†,‡] Mark J. Fernée,[†,‡] Serguei V. Goupalov,[§,∥] Paul Mulvaney,[⊥] Philippe Tamarat,[†,‡] and Brahim Lounis*[,†,‡]

[†]LP2N, Université de Bordeaux, F-33405 Talence, France, [‡]LP2N, Institut d'Optique and CNRS, F-33405 Talence, France, [§]Department of Physics, Jackson State University, Jackson, Mississippi 39217, United States, [∥]A.F. Ioffe Physico-Technical Institute, 194021 St. Petersburg, Russia, and [⊥]School of Chemistry, The University of Melbourne, Parkville, Victoria 3010, Australia

ABSTRACT We use nominally spheroidal CdSe nanocrystals with a zinc blende crystal structure to study how shape perturbations lift the energy degeneracies of the band-edge exciton. Nanocrystals with a low degree of symmetry exhibit splitting of both upper and lower bright state degeneracies due to valence band mixing combined with the isotropic exchange interaction, allowing active control of the level splitting with a magnetic field. Asymmetry-induced splitting of the bright states is used to reveal the entire 8-state band-edge fine structure, enabling complete comparison with band-edge exciton models.

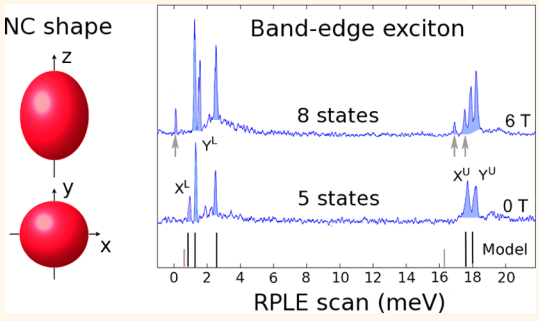

KEYWORDS: CdSe · single nanocrystal · PL · PLE · quantum dot · exciton fine structure

Semiconductor nanocrystals (NCs) prepared using low-cost colloidal syntheses present significant opportunities for a wide range of new and emerging technologies. In particular, these quantum dots could potentially be used in applications such as single-photon sources[1−3] and sources of entangled photon pairs.[4−7] The latter application is more demanding as it involves a biexciton−exciton emission cascade, requiring high biexciton quantum yields.[8−10] Nevertheless, heterostructure engineering has proven to be capable of fine-tuning the biexciton binding energy to help remove quantum "which path" information.[11] For a symmetric quantum dot, the generation of photon pairs proceeds through a bright doubly degenerate exciton state, and the two decay paths become "indistinguishable", ideally producing polarization-entangled photons.[12−14] One of the challenges in using self-assembled quantum dots in these applications is the restoration of the exciton degeneracy,[15−18] which requires a means of manipulating individual quantum state energies. Tuning of the excitonic energy levels has been demonstrated in NCs *via* the quantum-confined Stark effect,[19] but this technique is not state-specific, shifting the entire band-edge manifold of states uniformly.[20,21] Thus, techniques for moving individual quantum states can offer greater flexibility in the use of these systems.

Shape-anisotropy-induced splitting of the lowest energy bright exciton was reported for colloidal CdSe NCs.[22,23] Its observations offer insight into the physical properties of NC systems, which would be greatly improved by observations of the surrounding fine structure states that would reveal band ordering and shape information.[8] In fact, the eight-fold degenerate ground exciton state in spherical CdSe NCs is split by the electron−hole exchange interaction, which in wurtzite structure NCs is complemented by the built-in crystal field tending to separate the light-hole and heavy-hole excitons. This leads to the appearance of two doubly degenerate bright exciton states known as the $1^{U,L}$ states. Shape anisotropy can induce large splitting energies for the bright $1^{U,L}$ states[22] which are difficult to achieve using magnetic fields, due to the small g-factors.[24] Thus, NCs exhibiting shape anisotropy can potentially be used to provide access to

* Address correspondence to blounis@u-bordeaux1.fr.

Received for review September 2, 2014 and accepted October 20, 2014.

Published online October 20, 2014
10.1021/nn5049409

© 2014 American Chemical Society

each individual quantum state of the 8-state band-edge exciton, allowing comprehensive tests of various effective mass models.[23,25,26] However, technical hurdles have hitherto precluded experimental verification of the complete band-edge fine structure. This problem stems from multiple factors, such as insufficient spectral resolution, efficient energy relaxation between fine structure states, spectral degeneracies, and presence of dark states. Each of these problems can be solved individually, but the challenge remains to combine all the solutions in order to reveal the entire band-edge fine structure.

One such technical hurdle is to find a means to reliably engineer shape anisotropy into NC syntheses, as synthetic parameters usually favor highly symmetric growth. Shape variations have previously been reported for CdSe NCs with a wurtzite crystal structure[8] based on single NC photoluminescence (PL) spectroscopy. However, the apparently high cylindrical symmetry of these NCs seemed to preclude studying shape anisotropy in directions other than the dominant elongation *c*-axis. In addition, wurtzite structure crystals are characterized by an appreciable built-in crystal field, splitting the light-hole and heavy-hole sub-bands of the valence band. This splitting can be compensated in NCs with considerable shape elongation along the wurtzite axis but is quite large for spherical NCs. Fortunately, in the cubic zinc blende structure, the point of maximum spectral degeneracy is associated with purely spherical NCs,[27] as there is no crystal field. Thus, for zinc blende NCs, we expect that the band-edge fine structure should be highly sensitive to shape anisotropy, thus providing an excellent means for probing the symmetry of NC growth.

In this report, we study the polarization and magneto-optical properties of single CdSe NCs with a zinc blende structure that exhibits splitting of the bright upper and lower $1^{U,L}$ states. We use resonant photoluminescence excitation spectroscopy (RPLE) to probe both the upper and lower band-edge manifolds in order to correlate the lower 1^L state splitting with that of the upper 1^U state and reveal the entire ($1S_e$, $1S_{3/2}$) band-edge manifold of states for the first time. In addition, we demonstrate control of the bright state splitting with a magnetic field using PL spectroscopy.

RESULTS AND DISCUSSION

Spectroscopic Signature of Anisotropy-Induced Splitting. Previously, it has been shown that the zinc blende CdSe NCs used in this study can be described by a dominant spheroidal shape perturbation term, which divides the NCs into oblate and prolate shapes. These possess a lowest exciton energy state characterized by the total exciton angular momentum projection along the major deformation axis of either ±2 for oblate or 0 for prolate.[28] We find that it is the prolate shape for which splitting of the radiative doublet

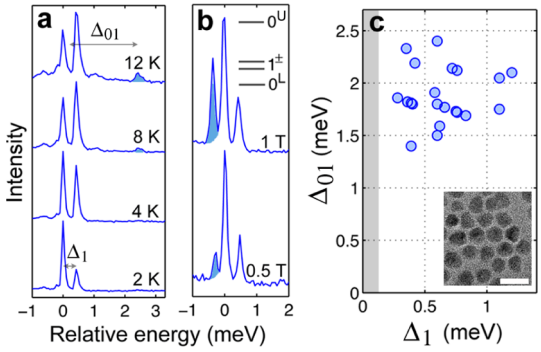

Figure 1. PL properties of the bright 1^L state splitting. (a) Temperature series revealing the emergence of the 0^U emission (shaded). (b) Applied magnetic field reveals the 0^L state (shaded). Inset: lower band-edge level assignments. (c) 1^L bright state splitting Δ_1 *vs* $1^L - 0^U$ energy difference Δ_{01} for 22 NCs (the shaded region represents the spectral resolution below which splittings cannot be resolved) (inset: TEM image of the NCs with a 20 nm scale bar indicated).

(associated with the 1^L bright state) is observed. Bright 1^L state splitting is not observed in NCs characterized with spectra indicating oblate geometry (~50% of the NCs). The properties of the split 1^L state are shown in Figure 1. The behavior of the spectral doublet with increasing temperature in Figure 1a indicates that the two spectral lines have similar oscillator strengths. In addition, an extra single state becomes thermally populated at higher temperature and often dominates the emission spectrum, consistent with its assignment to the bright 0^U state.[8,29,30] When a magnetic field is applied, a fourth spectral line appears to the red of the doublet (see Figure 1b), which is assigned to emission from the 0^L magnetically brightened dark state.[8,29]

In Figure 1c, we show the bright state 1^L splitting Δ_1 of 22 individual NCs as a function of the energy difference Δ_{01} between 0^U and 1^L states. Δ_1 has no characteristic energy but varies widely up to ~1 meV, in contrast to Δ_{01}, which is set by the isotropic electron–hole exchange interaction and should be similar for particles with similar volume.

Valence Band Mixing Model. There has been little discussion about the origin of the $1^{U,L}$ bright state splitting in NCs. Here we use relatively large NCs, which are well described by effective mass models. In this regime, the band-edge fine structure predicted effective mass models have been shown to converge with computationally intensive atomistic models[31] and are more insightful. Thus, possible discrepancies between the different approaches are avoided.[32,33] Two variants of the effective mass model have been proposed[23,25,26] that incorporate shape anisotropy in CdSe NCs with an important distinction being the physical origin of the bright state splitting. One model was based on the inclusion of an anisotropic exchange interaction term[23] to the effective mass Hamiltonian, while the other considered the effect of shape anisotropy on the valence band energies[25,26] (which is referred to as valence

band mixing) and neglected the anisotropic exchange interaction. Here we elaborate on why the valence band mixing term should be dominant and use this model to explain various properties observed in our experiment. Insight is obtained from the spin-Hamiltonian that determines the fine structure, which is given by[25]

$$\hat{H} = -\Delta(\hat{J}_z^2 - 5/4) - \bar{\eta}(\hat{\sigma}\cdot\hat{\mathbf{J}}) + C(\hat{J}_x^2 - \hat{J}_y^2) + \hat{H}_{AE} + \hat{H}_B$$

where $\hat{J}_\alpha$ ($\alpha = x,y,z$) are the matrices of projections of the $j = 3/2$ angular momentum operator and $\hat{\alpha}_\alpha$ are the Pauli matrices. The first term represents the dominant shape perturbation characterized by the energy Δ and defines the quantization axis (which coincides with the crystal *c*-axis in the case of wurtzite NCs); the second term corresponds to the isotropic electron–hole exchange with characteristic energy $\bar{\eta}$; the third term (proportional to *C*) represents the energy splitting due to shape anisotropy in a plane perpendicular to the quantization axis; $\hat{H}_{AE}$ corresponds to the anisotropic exchange interaction, and the final term, $\hat{H}_B$, represents the interaction with an external magnetic field. The anisotropic exchange term has a contribution to the total spin-Hamiltonian that is negligible in comparison to the valence band mixing term (proportional to *C*) because the hole confinement energy is an order of magnitude larger than the electron–hole exchange energy.[25] When the anisotropy-induced term proportional to *C* is combined with the isotropic exchange interaction, this results in the splittings of each of the $1^{U,L}$ doublets.

Magnetic Tuning of Fine Structure States. A magnetic field parallel to the quantization axis will cause the 1^L bright state splitting to increase, as a result of the Zeeman effect.[23] On the other hand, if we consider the elliptical anisotropy in a plane orthogonal to the quantization axis, then the effect of an in-plane magnetic field will depend on the orientation of the magnetic field relative to the main axes of the elliptical cross section. If the magnetic field is aligned with the long axis of the ellipse, the splitting will *increase* with increasing field, whereas for the field aligned with the short axis of the ellipse, it will *decrease*. These two cases are highlighted in Figure 2a,b using numerical simulations of the spin-Hamiltonian described above. We show in Figure 2c–f clear examples of both cases of splitting behavior in the PL spectra obtained in an applied magnetic field.

RPLE Reveals Higher Lying States. The anisotropy-induced splitting has been previously observed for the lowest energy bright state in wurtzite structure CdSe NCs.[22] This has been observed for the lowest energy bright state and is consistent with our observations (data not shown), although the orientation of the NCs relative to the optical axis can modify the apparent dipole angles. Here we would like to emphasize the role of the anisotropy-induced term resulting from the valence band mixing and proportional to *C*. Its

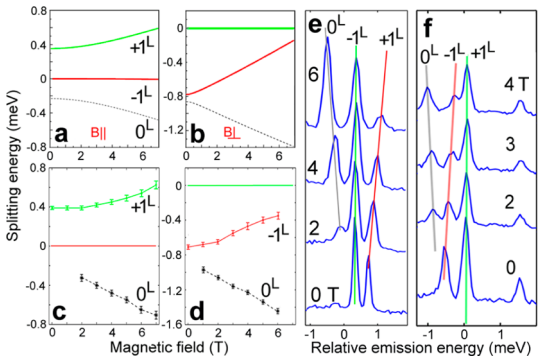

Figure 2. PL splitting energies in a magnetic field orthogonal to the quantization axis. (a) Theoretical prediction for the magnetic field parallel to the long axis of the in-plane elliptical anisotropy. (b) Behavior for B directed along the short axis of the elliptical anisotropy. The model corresponds to a prolate NC with an aspect ratio of 1.4 with in-plane deformations μ_{xy} = 0.06 and 0.15, respectively (as defined in ref 25). (c) Observed splitting behavior consistent with (a). (d) Observed splitting behavior consistent with (b). (e) Evolution of a single NC band-edge spectrum with the magnetic field at 4 K. The lines highlight the increased splitting shown in (c). (f) Evolution of a single NC band-edge spectrum with magnetic field at 8 K. The lines highlight the merging of the bright state doublet, similar to the behavior in (d). The 0^U state is also evident at higher energy.

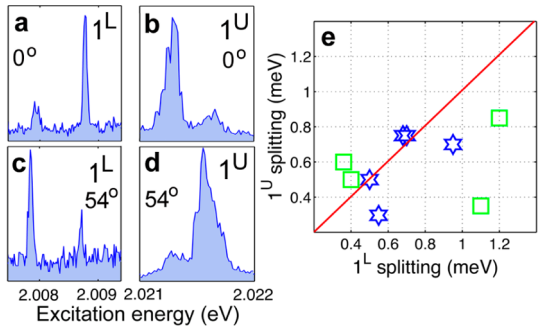

Figure 3. RPLE: Upper bright state splitting. (a,b) RPLE scans of the lower and upper bright state doublets excited with a vertically polarized laser. (c,d) PLE scans of the lower and upper bright states excited with a linearly polarized laser with the polarization at 54° relative to the vertical. (e) Splitting energies of the upper bright state relative to the lower bright state for zinc blende (squares) and wurtzite (stars) nanocrystals.

inclusion drastically affects the upper bright state splitting properties. In particular, the magnitude of the splitting induced by valence band mixing is predicted to be comparable for both the upper and lower bright states, and the polarization of the split components should be anticorrelated.[26] In contrast, a model that includes only anisotropic exchange interaction terms[23] predicts that the upper and lower bright state components have correlated polarizations and a significantly larger splitting of the upper bright state due to its larger oscillator strength.[23] The ability to distinguish between these two cases requires a means of detecting the upper bright state, which is generally not visible in PL spectra.

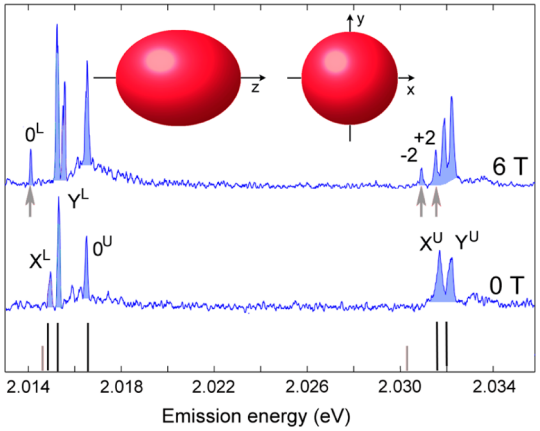

Figure 4. RPLE: Band-edge exciton structure. Excitation spectra for a prolate NC revealing the five bright states at zero field and the entire 8-state manifold in the presence of a magnetic field (arrows indicate dark states not visible at zero field) obtained at 2 K. Predicted peak positions at 0 T are indicated and correspond to a prolate NC with an average radius of 2.7 nm, aspect ratio of 1.3, and an asymmetric in-plane perturbation of 3% (inset: depiction of the spheroidal perturbations used to calculate the fine structure peak positions using solutions adapted from ref 25).

We search for higher lying states by conducting RPLE scans with a tunable laser source while monitoring the band-edge PL signal. With this technique, we are able to reveal higher lying nonluminescent bright states. For NCs exhibiting anisotropic splitting of the lower bright state 1^L, we also find a higher energy bright state 1^U doublet. Using polarized excitation, we directly probe this excited state dipole and find that it is also a linearly polarized doublet, as shown in Figure 3b,d. In addition, the upper and lower doublet polarizations are generally anticorrelated (see Figure 3a,b and c,d), matching the prediction of the model accounting for the anisotropy-induced term due to the valence band mixing.[26] We have studied a number of nanocrystals of both zinc blende and wurtzite crystal structure and found that the upper state splitting is always comparable to that of the lower bright state (see Figure 3e), which is also consistent with the predictions of the theory accounting for shape-induced valence band mixing.[25,26]

Resolving the Entire Band-Edge Fine Structure. The use of RPLE that derives its signal from the optical phonon replica[34−36] allows us to probe the entire band-edge exciton fine structure in a single laser scan. We show in Figure 4 that both the upper and lower bright states are observed with similar splitting energies, closely matching the theoretical model based on the solution of the spin-Hamiltonian for a NC with a mean radius of 2.7 nm and an aspect ratio of 1.3 along the dominant growth axis (quantization axis) and in-plane anisotropy of 3% deviation from a circular cross section (see inset in Figure 4). This indicates that only very small perturbations are required to produce the observed spectral signatures, suggesting that the dominant perturbation is still elongation along a single axis in the NCs used in this study. Thus, all the distinguishing characteristics of valence band mixing have been observed in our data, which comprise more than 10 individual NCs. Finally, we combine the PL excitation scan of an anisotropic NC in the presence of an applied magnetic field. The applied field induces mixing of the dark states (0^L and 2) with neighboring bright states[8,24,37] so that we are able to reveal the entire 8-state band-edge manifold of states in the 6 T spectrum of Figure 4. The splitting between the ± 2 states is attributed to Zeeman splitting in the external magnetic field[24] because the effect of shape anisotropy should be negligible on these states.[25]

CONCLUSION

In summary, we have used CdSe NCs with a zinc blende crystal structure to study morphological fluctuations around spherical symmetry. Spectral finger printing has been used to characterize NCs that exhibit splitting of their bright $1^{U,L}$ states. We have shown these have an essentially prolate geometry with a slight additional anisotropy. We have used RPLE to investigate the 1^U doublet, which allowed us to show that the splittings are attributable to valence band mixing in combination with the isotropic exchange interaction. We have shown that it is possible to have fine control over the split bright state energies using a magnetic field appropriately orientated in the deformation plane. One can, in principle, restore and break the degeneracy with an appropriately oriented magnetic field and selectively move individual bright states. Such control can be used to tailor the properties of entangled photon sources, control quantum interferences, and study energy relaxation between the band-edge states. Finally, we have used the bright state splitting induced by the shape anisotropy in conjunction with an applied magnetic field to experimentally visualize the entire 8-state band-edge for the first time. This provides exquisite experimental confirmation of the state ordering predicted by various models and provides a more rigorous spectroscopic example for comparing with any future models.

METHODS

The NCs used in this study[28] consisted of a 5.2 nm diameter CdSe core, made using a zinc blende synthesis, and overcoated with four monolayers of CdS and a single monolayer of ZnS, and were soluble in nonpolar organic solvents. These NCs were diluted with toluene/poly(methyl methacrylate) solution and spin-coated onto clean glass coverslips. High-resolution transmission electron microscope images (see inset Figure 1c) reveal that the NCs are *approximately* spherical but exhibit significant faceting and other shape fluctuations toward lower symmetry.

The sample is mounted in a magneto-optical cryostat capable of providing magnetic fields up to 7 T and temperatures as low

as 2 K, with samples immersed in a low-pressure He exchange gas atmosphere. A home-built scanning confocal microscope is used to image single NCs excited with the 532 nm line of a cw frequency-doubled Nd:YAG laser. It is based on a high numerical aperture objective housed in a magnetic cryostat together with the sample and a piezoscanner, which raster scans the sample in order to provide an image. The objective axis is perpendicular to the magnetic field, allowing magneto-optical studies in the Voigt configuration. The emitted photons are filtered from the scattered excitation light by a low-pass filter (60 nm fwhm) and sent to a single-photon counting avalanche photodiode and a spectrometer.

PL measurements are conducted using a 532 nm laser as a nonresonant pump, and the red-shifted PL is dispersed in the spectrometer with a spectral resolution of 120 μeV. Low pump powers at or below 100 nW are used to prevent photophysical ionization that results in trion emission.[28]

RPLE measurements are conducted using a tunable cw dye ring laser operating with a sulforhodamine B dye. Tuning is accomplished by rotating an intracavity birefringent filter using a computer-driven stepper motor. The output of the dye laser is passed through a noise eater to produce a constant intensity over the entire scan range. Stokes shifted fluorescence is collected with an avalanche photodiode using an angle-adjusted ultrasteep edge filter to remove laser scatter.

Conflict of Interest: The authors declare no competing financial interest.

Acknowledgment. This work was funded by the Agence Nationale de la Recherche, Région Aquitaine, the European Research Council and the Institut Universitaire de France. S.V. G. was supported by the Research Corporation for Science Advancement (Award No. 20081), the Russian Foundation for Basic Research, and the National Science Foundation.

REFERENCES AND NOTES

1. Michler, P.; Kiraz, A.; Becher, C.; Schoenfeld, W. V.; Petroff, P. M.; Zhang, L. D.; Hu, E.; Imamoglu, A. A Quantum Dot Single-Photon Turnstile Device. *Science* **2000**, *290*, 2282–2285.
2. Lounis, B.; Bechtel, H. A.; Gerion, D.; Alivisatos, P.; Moerner, W. E. Photon Antibunching in Single CdSe/ZnS Quantum Dot Fluorescence. *Chem. Phys. Lett.* **2000**, *329*, 399–404.
3. Brokmann, X.; Messin, G.; Desbiolles, P.; Giacobino, E.; Dahan, M.; Hermier, J. P. Colloidal CdSe/ZnS Quantum Dots as Single-Photon Sources. *New J. Phys.* **2004**, *6*, 99.
4. Benson, O.; Santori, C.; Pelton, M.; Yamamoto, Y. Regulated and Entangled Photons from a Single Quantum Dot. *Phys. Rev. Lett.* **2000**, *84*, 2513–2516.
5. Stevenson, R. M.; Young, R. J.; Atkinson, P.; Cooper, K.; Ritchie, D. A.; Shields, A. J. A Semiconductor Source of Triggered Entangled Photon Pairs. *Nature* **2006**, *439*, 179–182.
6. Akopian, N.; Lindner, N. H.; Poem, E.; Berlatzky, Y.; Avron, J.; Gershoni, D.; Gerardot, B. D.; Petroff, P. M. Entangled Photon Pairs from Semiconductor Quantum Dots. *Phys. Rev. Lett.* **2006**, *96*, 130501.
7. Moreau, E.; Robert, I.; Manin, L.; Thierry-Mieg, V.; Gérard, J. M.; Abram, I. Quantum Cascade of Photons in Semiconductor Quantum Dots. *Phys. Rev. Lett.* **2001**, *87*, 183601.
8. Louyer, Y.; Biadala, L.; Trebbia, J. B.; Fernee, M. J.; Tamarat, P.; Lounis, B. Efficient Biexciton Emission in Elongated CdSe/ZnS Nanocrystals. *Nano Lett.* **2011**, *11*, 4370–4375.
9. Park, Y. S.; Malko, A. V.; Vela, J.; Chen, Y.; Ghosh, Y.; Garcia-Santamaria, F.; Hollingsworth, J. A.; Klimov, V. I.; Htoon, H. Near-Unity Quantum Yields of Biexciton Emission from CdSe/CdS Nanocrystals Measured Using Single-Particle Spectroscopy. *Phys. Rev. Lett.* **2011**, *106*, 187401.
10. Zhao, J.; Chen, O.; Strasfeld, D. B.; Bawendi, M. G. Biexciton Quantum Yield Heterogeneities in Single CdSe (CdS) Core (Shell) Nanocrystals and Its Correlation to Exciton Blinking. *Nano Lett.* **2012**, *12*, 4477–4483.
11. Sitt, A.; Salla, F. D.; Menagen, G.; Banin, U. Multiexciton Engineering in Seeded Core/Shell Nanorods: Transfer from Type-I to Quasi-Type-II Regimes. *Nano Lett.* **2009**, *9*, 3470–3476.
12. Graham, T. C. M.; Curran, A.; Tang, X.; Morrod, J. K.; Prior, K. A.; Warburton, R. J. Direct and Exchange Coulomb Energies in CdSe/ZnSe Quantum Dots. *Phys. Status Solidi B* **2006**, *243*, 782–786.
13. Santori, C.; Fattal, D.; Pelton, M.; Solomon, G. S.; Yamamoto, Y. Polarization-Correlated Photon Pairs from a Single Quantum Dot. *Phys. Rev. B* **2002**, *66*, 045308.
14. Ulrich, S. M.; Strauf, S.; Michler, P.; Bacher, G.; Forchel, A. Triggered Polarization-Correlated Photon Pairs from a Single CdSe Quantum Dot. *Appl. Phys. Lett.* **2003**, *83*, 1848–1850.
15. Stevenson, R. M.; Young, R. J.; See, P.; Gevaux, D. G.; Cooper, K.; Atkinson, P.; Farrer, I.; Ritchie, D. A.; Shields, A. J. Magnetic-Field-Induced Reduction of the Exciton Polarization Splitting in InAs Quantum Dots. *Phys. Rev. B* **2006**, *73*, 033306.
16. Ding, F.; Singh, R.; Plumhof, J. D.; Zander, T.; Křápek, V.; Chen, Y. H.; Benyoucef, M.; Zwiller, V.; Dörr, K.; Bester, G.; *et al.* Tuning the Exciton Binding Energies in Single Self-Assembled InGaAs/GaAs Quantum Dots by Piezoelectric-Induced Biaxial Stress. *Phys. Rev. Lett.* **2010**, *104*, 067405.
17. Kowalik, K.; Krebs, O.; Golnik, A.; Suffczynski, J.; Wojnar, P.; Kossut, J.; Gaj, J. A.; Voisin, P. Manipulating the Exciton Fine Structure of Single CdTe/ZnTe Quantum Dots by an In-Plane Magnetic Field. *Phys. Rev. B* **2007**, *75*, 195340.
18. Bennett, A. J.; Pooley, M. A.; Stevenson, R. M.; Ward, M. B.; Patel, R. B.; Boyer de la Giroday, A.; Sköld, N.; Farrer, I.; Nicoll, C. A.; Ritchie, D. A.; *et al.* Electric-Field-Induced Coherent Coupling of the Exciton States in a Single Quantum Dot. *Nat. Phys.* **2010**, *6*, 947–950.
19. Empedocles, S. A.; Bawendi, M. G. Quantum-Confined Stark Effect in Single CdSe Nanocrystallite Quantum Dots. *Science* **1997**, *278*, 2114–2117.
20. Le Thomas, N.; Herz, E.; Schops, O.; Woggon, U.; Artemyev, M. V. Exciton Fine Structure in Single CdSe Nanorods. *Phys. Rev. Lett.* **2005**, *94*, 016803.
21. Fernée, M. J.; Littleton, B. N.; Rubinsztein-Dunlop, H. Detection of Bright Trion States Using the Fine Structure Emission of Single CdSe/ZnS Colloidal Quantum Dots. *ACS Nano* **2009**, *3*, 3762–3768.
22. Htoon, H.; Furis, M.; Crooker, S. A.; Jeong, S.; Klimov, V. I. Linearly Polarized 'Fine Structure' of the Bright Exciton State in Individual CdSe Nanocrystal Quantum Dots. *Phys. Rev. B* **2008**, *77*, 035328.
23. Htoon, H.; Crooker, S. A.; Furis, M.; Jeong, S.; Efros, A. L.; Klimov, V. I. Anomalous Circular Polarization of Photoluminescence Spectra of Individual CdSe Nanocrystals in an Applied Magnetic Field. *Phys. Rev. Lett.* **2009**, *102*, 017402.
24. Biadala, L.; Louyer, Y.; Tamarat, P.; Lounis, B. Band-Edge Exciton Fine Structure of Single CdSe/ZnS Nanocrystals in External Magnetic Fields. *Phys. Rev. Lett.* **2010**, *105*, 157402.
25. Goupalov, S. V. Anisotropy-Induced Exchange Splitting of Exciton Radiative Doublet in CdSe Nanocrystals. *Phys. Rev. B* **2006**, *74*, 113305.
26. Goupalov, S. V. Anomalous Polarization of the Photoluminescence from Anisotropic Colloidal CdSe Nanocrystals Subject to External Magnetic Fields. *Phys. Rev. B* **2009**, *79*, 233301.
27. Efros, A. L.; Rosen, M.; Kuno, M.; Nirmal, M.; Norris, D. J.; Bawendi, M. Band-Edge Exciton in Quantum Dots of Semiconductors with a Degenerate Valence Band: Dark and Bright Exciton States. *Phys. Rev. B* **1996**, *54*, 4843–4856.
28. Fernée, M. J.; Sinito, C.; Louyer, Y.; Potzner, C.; Nguyen, T.-L.; Mulvaney, P.; Tamarat, P.; Lounis, B. Magneto-optical Properties of Trions in Non-blinking Charged Nanocrystals Reveal an Acoustic Phonon Bottleneck. *Nat. Commun.* **2012**, *3*, 1287.
29. Fernée, M. J.; Tamarat, P.; Lounis, B. Cryogenic Single-Nanocrystal Spectroscopy: Reading the Spectral Fingerprint of Individual CdSe Quantum Dots. *J. Phys. Chem. Lett.* **2013**, *4*, 609–618.

30. Moreels, I.; Raino, G.; Gomes, R.; Hens, Z.; Stoferle, T.; Mahrt, R. F. Band-Edge Exciton Fine Structure of Small, Nearly Spherical Colloidal CdSe/ZnS Quantum Dots. *ACS Nano* **2011**, *5*, 8033–8039.
31. Fernee, M. J.; Tamarat, P.; Lounis, B. Spectroscopy of Single Nanocrystals. *Chem. Soc. Rev.* **2014**, *43*, 1311–1337.
32. Sewall, S. L.; Cooney, R. R.; Kambhampati, P. Experimental Tests of Effective Mass *vs.* Atomistic Pictures of Quantum Dot Electronic Structure. *Appl. Phys. Lett.* **2009**, *94*, 243118.
33. Tyagi, P.; Cooney, R. R.; Sewall, S. L.; Sagar, D. M.; Saari, J. I.; Kambhampati, P. Controlling Piezoelectric Response in Semiconductor Quantum Dots *via* Impulsive Charge Localization. *Nano Lett.* **2010**, *10*, 3062–3067.
34. Biadala, L.; Louyer, Y.; Tamarat, P.; Lounis, B. Direct Observation of the Two Lowest Exciton Zero-Phonon Lines in Single CdSe/ZnS Nanocrystals. *Phys. Rev. Lett.* **2009**, *103*, 037404.
35. Fernée, M. J.; Plakhotnik, T.; Louyer, Y.; Littleton, B. N.; Potzner, C.; Tamarat, P.; Mulvaney, P.; Lounis, B. Spontaneous Spectral Diffusion in CdSe Quantum Dots. *J. Phys. Chem. Lett.* **2012**, *3*, 1716–1720.
36. Fernée, M. J.; Sinito, C.; Louyer, Y.; Tamarat, P.; Lounis, B. The Ultimate Limit to the Emission Linewidth of Single Nanocrystals. *Nanotechnology* **2013**, *24*, 465703.
37. Nirmal, M.; Norris, D. J.; Kuno, M.; Bawendi, M. G.; Efros, A. L.; Rosen, M. Observation of the Dark Exciton in CdSe Quantum Dots. *Phys. Rev. Lett.* **1995**, *75*, 3728–3731.